Photophysics of a Bridged 7-Diethylamino-4-methyl-coumarin C102: Studying the Hydrogen Bonding Effect by Time Resolved Stimulated Emission

F. Morlet-Savary,* C. Ley, P. Jacques, and J. P. Fouassier

Département de Photochimie Générale, CNRS UMR n°7525, Ecole Nationale Supérieure de Chimie de Mulhouse, 3 Rue Alfred Werner, 68093 Mulhouse Cedex, France

Received: February 27, 2001; In Final Form: September 18, 2001

The time-resolved stimulated emission of a 7-diethylamino-4-methyl-coumarin dye, Coumarin 102 (C102), was investigated in polar and hydroxylic solvents. Analysis of these spectroscopic measurements using semiempirical solvent polarity scales ($E_T(30)$, Kamlet and Taft) showed that the stabilization of the excited singlet state is mainly governed by dipolar and hydrogen bonding interactions. This particuliar behavior was reflected by a good adequacy between the present measured solvation times and the microscopic (or molecular) relaxation times related to both the Debye relaxation time τ_D (dielectric continuum model) and the Kirkwood factor g_k, which expresse the degree of short range order in the liquid. These data were compared with the ones obtained for thioxanthone via pump−probe experiments and other data available in the literature.

Introduction

In the liquid phase, the change in solute dipole moment induced by electronic excitation initiates a complex solvation process in which the energy of the dipole is reduced by solvent reorientation, thus resulting in a shift of the electronic transition frequencies.[1−3] The theoretical study was pioneered by Bakshiev and Mazurenko[4−6] and recently by Bagchi et al.,[7] van der Zwan et al.,[8] and Maroncelli et al.[9]

The electronic state solvation, i.e., the response of the solvent to the electronic structure of a solute, can be classified into three categories: polar solvation, as a result of the interaction between the solvent dipoles and the solute charge distribution; non polar solvation, produced by repulsive and dispersion forces; and "specific" interactions, which most often result from hydrogen bonding.[10] The dynamics of polar solvation was extensively studied[1,3] in recent years by using fluorescent probes such as coumarin dyes, mainly Coumarin 153 (C153), Coumarin 102 (C102), and other molecular probes. Recently, information on nonpolar solvation dynamics also was gained.[11−13] However, few results were reported on the dynamics of solvation by hydrogen bonding and about the lifetime of hydrogen−solvent bonds. Hydrogen bonding with the solvents was recognized as an important interaction with a large variety of solutes in protic solvents.[10] Several research groups observed changes in solvation dynamics of DMABN,[14] an oxazine derivative,[15−18] 9,9′-bianthryl,[19] and resorufin,[20] which were attributed to solvent hydrogen bonding. Apart from these few examples, the problem is a lack of systems in which hydrogen bond solvation can be clearly distinguished from other solvation processes.

For example, in C153, it is assumed that no intramolecular processes take place apart from vibrational relaxation; thus, when this is completed the remaining transient Stokes shift accounts for solvation. However, there were several discussions on possible intramolecular contributions to the time-resolved dynamic Stokes shift of C153. The state-of-the-art can be summed up as follows. Agmon[21] suggested that "inhomogeneous" spectral relaxation may explain earlier picosecond experiments carried out by Maroncelli et al.[22] In addition, Blanchard et al. [23] reported an "anomalous" behavior of this dye in "slow" solvents and expressed doubts about its suitability for probing solvation. More recent results reported by Kovalenko et al.[24] and obtained with a higher time resolution show that they are not fully consistent with a relaxation process resulting from pure solvation and may indicate the occurrence of an intramolecular process. More precisely, the semiempirical calculations[25] predict the presence of two closely spaced singlet states as well as several triplet states that are consistent with the experimental data of Blanchard et al.[23]

Most of the experimental studies in liquid phase are based on time dependent fluorescence shift (TDFS) of the excited states of a probe examined by time-resolved up-conversion of fluorescence in ultrafast studies or "conventional" time photon counting technique in fast processes. These techniques make it possible to obtain kinetic traces of the fluorescence intensity at selected wavelengths. After scaling to the steady-state time integral, the traces provide a means for reconstructing the fluorescence spectra as a function of time.[22] At the first glance, this method should be characterized by an excellent time resolution. However, the up-conversion signal is a convolution of the time- and frequency-dependent fluorescence intensity with the spectrotemporal apparatus function.

A complementary approach to these fluorescence experiments based on transient absorption and using a white light continuum was suggested by Bingemann et al.[26,27] In the fluorescence band where stimulated emission leads to the amplification of the continuum, the stimulated emission spectrum is measured. This technique may improve results compared to other techniques mentioned above for the following reasons:[26,27] (i) the temporal and spectral evolutions are also independent,[28] (ii) there is no need to reconstruct the stimulated emission spectrum as a function of time[22] and the spectral resolution is only limited by the spectrograph of the detection system. However, the technique has some limits as stressed by Bingeman et al.[26] First of all, the transient spectra are a sum of different contributions, especially excited state absorption and saturation of ground state absorption, which spectrally overlay the stimulated emission. Also, there must be a strong overlap between the probe spectrum and the fluorescence emission band. Despite these limits, the technique was applied to revisit the excited state dynamics of several fluorescent probes used for studying solvation dynamics in polar solvents and especially that of C153.[24,23]

In the present study, the solvation dynamics, especially the H-bonding contribution, of a particular 7-diethylamino-4-methyl-

* To whom correspondence should be addressed. E-mail: f.morlet-savary@uha.fr.

10.1021/jp010753n CCC: $20.00
Published on Web 11/16/2001

coumarin dye (C102) were investigated in several solvents via time-resolved stimulated emission. This dye is similar in structure to the well-known C153, which is extensively used as a probe in solvation dynamics studies,[29,30] but characterized by a smaller dipolar moment variation due to a substantially weaker intramolecular charge transfer (ICT) and the presence of a methyl group in place of a strongly electron-withdrawing trifluoromethyl group for C153. C102 was also used as a probe in studies of solvation dynamics[31−33] but to a lesser extent compared to its well-known analogue.

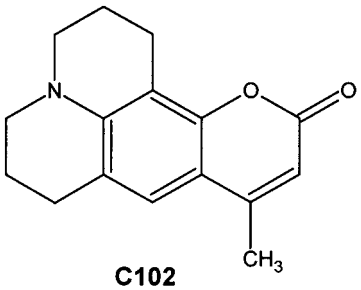

C102

In homogeneous solvents, C102 exhibits a marked red shift of both emission and absorption spectra on going from hydrocarbon solvents to an aqueous medium, from 361 nm in hydrocarbons to 396 nm in water for absorption, while emission shifts from 407 to 489 nm.[34] The other reason to use C102 as a probe was that the bridging of the nitrogen atom will hinder the rotations and conformation stages: large structural rearrangement will be prevented and the solvent cage will be perturbed mainly by the dipole moment change, thus allowing the observation of a pure cage relaxation process. From this point of view, C102 will be a nearly ideal probe.

It is known from solvent effect experiments[35] that C102 seems to be more sensitive to specific interactions, such as hydrogen bonding, than is its homologue C153 if a solvatochromic parameter approach is used.[36−38] Moog et al.[35] suggested an additional interaction between coumarins and alcohols. The extent of these specific interactions viewed as an influence in electronic transition is more conspicuous for C102 than for C153 because of its greater hydrogen bonding ability. This additional interaction is left out in the reaction field approach, such deviations being attributed to the presence of hydrogen bonding interactions.[39]

Hydrogen bonds are affected when proton transfer frequently takes place or when hydrogen bonds may be broke. These phenomena occur on ultrafast time scales and thus are a class of chemical reaction dynamics within the expanding field of femtochemistry in gas phase[40] or in condensed medium. This latter aspect was brought to light by very recent works concerned with the dynamics of hydrogen bonded complexes of C102 induced by electronic excitation through ultrafast vibrational or optical pump−probe or grating experiments.[41−44] The evolution of H-bonded complexes resulting from the interaction of C102 with hydrogen donors exhibits two stages: (a) a hydrogen bond cleavage within 200 fs, which means that the complex evolves with a finite lifetime toward a non H-bonded state, (b) a reorganization of the molecular fragments and the surrounding solvent shell, which may lead to the reformation of the hydrogen bond at the carbonyl group on the tens of picoseconds time scale in hydrogen bond donating solvents.[30]

Experimental data were previously gathered in our laboratory by using the thioxanthone (TX) molecule as a probe to study the hydrogen bonding effect on the solvation dynamics of an excited state.[45] In that paper, the $T_1 \rightarrow T_n$ transition depicted hydrogen bonding in the solvation process of the excited triplet state T_1 occurring in hydroxylic solvents through the dynamic shift of this electronic transition. The aim of the present study was to use C102 in its first excited singlet state S_1 as a probe to investigate the hydrogen bond solvation in hydroxylic solvents on the picosecond time scale. The objectives were to compare the measured specific relaxation times of C102 to those collected for TX and other probes mentioned in the literature and to see if the complex electronic structure and intramolecular energy dissipation characteristics of coumarins, as reported by Blanchard et al.[23,25] for C153, still play a role in a similar rigid coumarin dye such as C102.

Experimental Section

Chemicals. The structural formula of coumarin derivative C102 is 2,3,6,7-tetrahydro-9-methyl-1H,5H,11H-[1]benzopyrano[6,7,8−cy]quinolizin-11-one; (CAS number, C102:41267-76-9). Coumarin dye C102 was purchased from Exciton (laser grade) and used without further purification. The experiments were carried out in spectrophotometric and HPLC grade solvents. The experiments were carried out in argon-saturated solutions unless otherwise stated.

Time-Resolved Absorption Setup. The transients were analyzed by using a typical device of time-resolved absorption spectroscopy with a picosecond light source excitation. The latter was based on the spectroscopic pump probe. The basic principle consisted in preparing a transient species with a short laser pulse (pump pulse) and passing a white light pulse (probe pulse) through the sample so that a transient absorption spectrum could be recorded. The picosecond pulses were delivered by a passively actively mode locked Nd:YAG laser. The fundamental (1064 nm) and the third harmonic (355 nm) emissions were used respectively to generate a white light continuum probe from a D_2O/H_2O mixture and to excite the sample in solution, respectively. The white light was collected, collimated by a set of achromatic lenses, and sent onto a large band beam splitter to illuminate both sample and reference cells. The transmitted light was focused by suitable lenses and injected into fiber optics directly connected to the dispersive element of the double diode array multichannel analyzer. The solution was caused to flow through two cells (2 mm-optical pathway): the reference cell (non-excited) and the sample cell (excited). A delay of up to 6 ns could be achieved between the pump and probe pulses by using a computer-controlled micrometer translation stage. To obtain a transient absorption spectrum, signals were averaged over 400 laser shots with the excitation beam and another 400 laser shots without the excitation beam. The laser excitation energy was ca. 250 μJ while the excitation beam diameter was 2 mm in diameter, the probe one was 1 mm. The transient absorbance was calculated according to

$$\mathrm{Abs} = \log\left\{\frac{I^0_{\mathrm{sample}}}{I^0_{\mathrm{ref}}}\frac{I^{\mathrm{e}}_{\mathrm{ref}}}{I^{\mathrm{e}}_{\mathrm{sample}}}\right\} \qquad (1)$$

where I^0_{ref} and I^0_{sample} refer to the intensities measured through reference and sample cells with excitation off, $I^{\mathrm{e}}_{\mathrm{ref}}$ and $I^{\mathrm{e}}_{\mathrm{sample}}$ to the ones measured with excitation on. The transient absorbance $\mathrm{Abs}(t, \lambda_{\mathrm{obs}})$ obtained from the transient spectra at an observed wavelength λ_{obs} is fitted according to

$$\mathrm{Abs}(\mathrm{t}, \lambda_{\mathrm{obs}}) = \int_0^t I(\tau)F(t-\tau)\mathrm{d}\tau \qquad (2)$$

where $F(t)$ is the molecular kinetics, $I(\tau)$ is the instrument response function produced by the convolution of the pump and

SCHEME 1

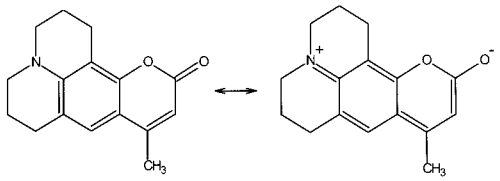

SCHEME 2

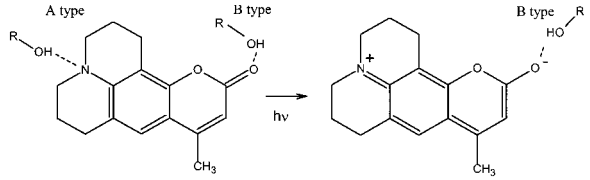

probe light and is assumed to have the analytical form of a Gaussian with a pulse width of σ.

$$I(t) = (1/\sqrt{2\pi\sigma})\exp\left[-\frac{(t-t_0)^2}{2\sigma^2}\right] \quad (3)$$

Here t_0 is the position of the peak of the Gaussian. This time t_0 corresponds to the maximum overlap between the pump and probe pulses and may be slightly wavelength dependent. For this reason, the transient spectra or kinetics are time referenced toward the mechanical origin of the setup, instead of t_0. To obtain the parameters t_0 and σ, the build-up of the $S_1 \rightarrow S_n$ transition of pyrene (or anthracene), which can be considered as instantaneous phenomena under picosecond excitation, is measured. The values of σ and t_0 are ca. 28 ps and ca. 100 ps, respectively. Such value for σ leads to a rise time of 50 ps for the present setup.

The calculated absorbance Abs(t) (relation 3) was then compared to the experimental one through the sum of the square of the residual res(t)

$$\mathrm{res}(t) = \sum_t [\mathrm{Abs}_{\mathrm{exp}}(t) - \mathrm{Abs}_{\mathrm{calc}}(t)]^2 \quad (4)$$

The best fit was obtained for a minimum value of res(t), which yields the optimum parameter values for the $F(t)$ molecular kinetics function.

Finally, the time resolution is determined by monitoring the $T_1 \rightarrow T_n$ absorption build up for benzophenone in acetonitrile solution. In relation 2, the $F(t)$ molecular kinetics function is

$$F(t) = \left[1 - \exp\left(-\frac{t}{\tau}\right)\right] \quad (5)$$

The fit with the experimental data yielded a value of 10 ± 5 ps for τ under the typical experimental conditions. Thus, the resulting time resolution of the experimental setup was estimated to be better than 10 ps.

Results and Discussion

As shown in Scheme 1, the mesomeric form of C102 leads to a negative character of the carbonyl oxygen, so that one may expect hydrogen bonding between solute and solvent molecules in both ground and excited states on this moiety. This negative character of the carbonyl bond is enhanced in the excited state, since intramolecular charge transfer (ICT) seems to occur in coumarin dyes after photoexcitation.

Effectively, results suggest that the low-lying emissive excited state of the aminocoumarins is postulated to be ICT in

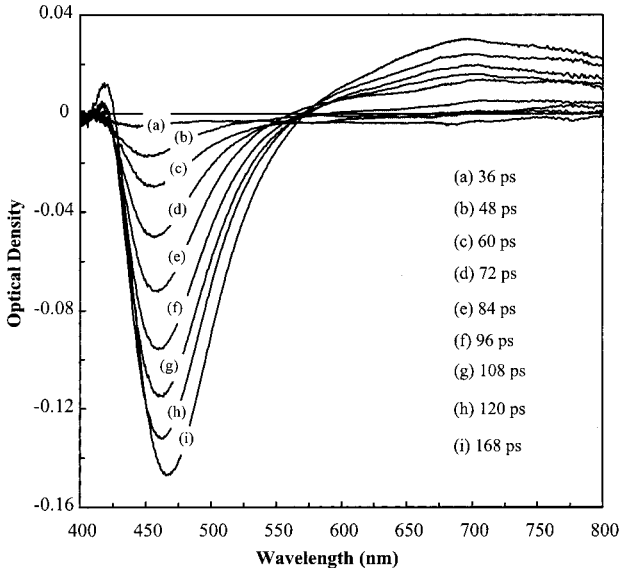

Figure 1. Transient spectra of C102 in 1-propanol taken at different pump−probe delays: from 36 to 168 ps.

character.[34] The most important fact to note is that the magnitude of the change in dipole moment ($\Delta\mu$) on electronic excitation is the most decisive parameter that determines the nature of the emitting state (locally excited or ICT). A calculated value of 3.66 D for $\Delta\mu$ is reported in the AM1 study of the electronic structure of coumarins.[25] Other experimental works, such as time-resolved microwave dielectric absorption measurements,[46] yield 3.0 D in benzene and 3.8 D in 1,4-dioxane, respectively. From these measurements, Samanta et al.[46] conclude that the fluorescence of C102 originates from a more polar state than the ground state and not from a high dipolar zwitterionic or ICT state.

It is known from quantum mechanical calculations based upon empirical methods[47−50] that coumarin dyes have a strong charge density on the carbonyl oxygen. However, the nitrogen atom in the julolidine group also has a negative charge according to these semiempirical calculations: this group may also function as a hydrogen acceptor site (Scheme 2, A-type[51]). The electron pair of the nitrogen atom will, however, be conjugated with the π-electron orbitals: one may expect that a possible attachment of a hydrogen donor on the nitrogen atom will lead to strong changes in the electronic energies of the π-orbitals. On the other hand, the carbonyl oxygen electron density is also present in the molecular plane, and these lone pairs are strong candidates for the formation of hydrogen bonds (Scheme 2, B-type[51]). After photoexcitation, A-type hydrogen bonds are loosened while B-type hydrogen bonds are strengthened as shown in Scheme 2.

The transient spectra of C102 in 1-propanol solvent, as an example of typical results, measured at different pump−probe delays, are shown in Figure 1. These spectra exhibit the following features: (i) a strong negative band centered at ca. 450 nm and (ii) a small broad band absorption in the 550−800 nm region. The negative optical density corresponds to a stimulated emission while a positive optical density indicates an excited-state absorption. This figure shows the transient absorption and emission for a pump−probe delay up to 168 ps (spectrum (i), Figure 1); at longer delays, no further changes are observed in the spectral shape and in the optical density. Also, the experimental data (Figure 1) indicate that the dominant

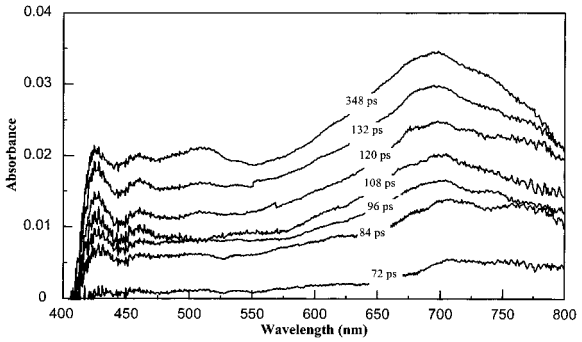

Figure 2. Transient absorption spectra of C102 in 1-propanol solution corrected from the stimulated emission.

response is a stimulated emission. The kinetic aspects of the transient absorption and the stimulated emission will be considered in the following section.

The Transient Absorption Band. Only a few papers are concerned with the transient absorption of coumarin dyes (C153,[52] C102,[53] and C1[54,55]) submitted to pulse radiolysis and nanosecond laser excitation, or more recently picosecond pump−probe spectroscopy studies (C102 and C1[56]).

The two major contributions, i.e., the stimulated emission and the transient absorption as well as other contributions from the transient spectra, should be separately considered. The stimulated emission was subtracted from the time-resolved spectra by using a log-normal shape function $\epsilon(\nu)$ as defined by[57]

$$\epsilon(\nu) = \left\{\epsilon_0 \exp\left[-\mathrm{Ln}\,2\left(\frac{1}{\beta}\mathrm{Ln}\left[1+\frac{2\beta(\nu-\nu_0)}{\Delta}\right]\right)^2\right]\right\} \quad (6a)$$

if $\alpha > -1$ or

$$\epsilon(\nu) = 0 \quad (6b)$$

if $\alpha \leq -1$ with

$$\alpha = \frac{2\beta(\nu-\nu_0)}{\Delta}$$

where parameters ϵ_0, ν_0, β, and Δ are peak height, peak frequency, asymmetry and spectral bandwith parameters, respectively. This log-normal function describes an asymmetric line shape which reduces to a Gaussian shape function at the limit $\beta = 0$. The optimum values for the parameters ϵ_0, ν_0, β, and Δ are obtained through least-squares analysis restricted to the spectral region of the stimulated emission band since (i) no substructure is observed and (ii) stimulated emission is the predominant process.

The final result (transient absorption spectra) for C102 in 1-propanol solution is shown in Figure 2. As mentioned above, the transient absorption is weak and broad, with a maximum at ca. 690 nm. After a similar treatment, the same transient absorption spectra were observed in the other hydroxylic solvents considered (nos. 5−11), e.g., 1-butanol or ethanol, with an absorption maximum at ca. 690 nm. For the rest of the discussion, emphasis will be laid on the results obtained in 1-propanol.

Figure 3 shows the transient absorption monitored at 690 nm for C102 in 1-propanol. The build up of the absorption is achieved in roughly 100 ps. Over this delay, which corresponds to the overlap between pump and probe pulses, the transient absorption remains the same in the time range considered in Figure 3. This kinetic trace is fitted according to relation 2 where

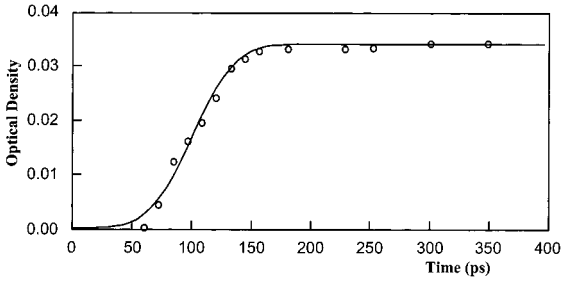

Figure 3. Transient absorption of C102 monitored at 690 nm and fitted according to a monoexponential rise. Experimental (○), calculated (full line). The following parameters were used: $A = 0.034$; $\sigma = 28$ ps; $\tau \leq 1$ ps; res $= 2.203 \times 10^{-5}$.

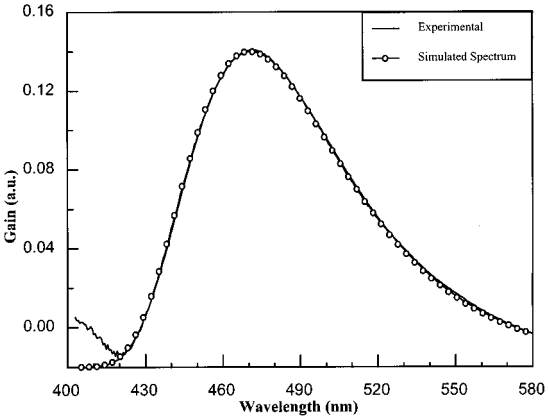

Figure 4. Stimulated emission spectrum of C102 in 1-propanol taken at $\Delta t = 350$ ps and fitted with a log-normal distribution. Fitting parameters are: $\epsilon_0 = 0.16$, $\Delta = 3.22 \times 10^3$ cm^{-1}, $\nu_0 = 21230$ cm^{-1}, $\beta = -0.33$.

the molecular kinetic function $F(t)$ stands for a monoexponential rise (relation 5) and τ is the lifetime of the process. After convolution of relation 5 with the apparatus function, the fit with the experimental data gives a lifetime shorter than 5 ps (time accuracy of the apparatus), which means that the process is faster than the time resolution of the setup. Yip et al.[56] observed a broad band absorption for C102 in water, centered however at ca. 630 nm, which they ascribed to a triplet−triplet absorption, in agreement with data from pulse radiolysis experiments where Priyadasini et al.[52,53] found the triplet−triplet absorption maximum at ca. 600 nm for the C153 and C102 compounds in benzene solution. Another fact derived from Figure 2 is that the maximum of the transient absorption exhibits a blue shift as the pump−probe delay increases. Conversely, a red shift was observed for the stimulated emission band (Figure 1). This last remark as well as the instantaneous absorption process (less than 5 ps) confirm that both absorption and stimulated emission originate from the same excited state S_1 and that the present transient absorption centered at ca. 690 nm may be ascribed to the $S_1 \rightarrow S_n$ transition. Unfortunately, it is not possible to ascertain whether both emission and absorption shifts are correlated in time, due to the poor quality of the transient absorption spectra, and not to a signal-to-noise ratio point of view, but from a spectral one. In other words, one cannot determine the wavelength of absorption maximum with a sufficient accuracy to build a shift correlation function, since the absorption band covers a large spectral range. However, the analysis of the transient absorption of C102 needs further experiments and will be the subject of a forthcoming paper.[58] The major result is that the transient absorption is flat and structureless in the 420−550 nm spectral range. Accordingly, the stimulated emission band is not distorted (or modulated)

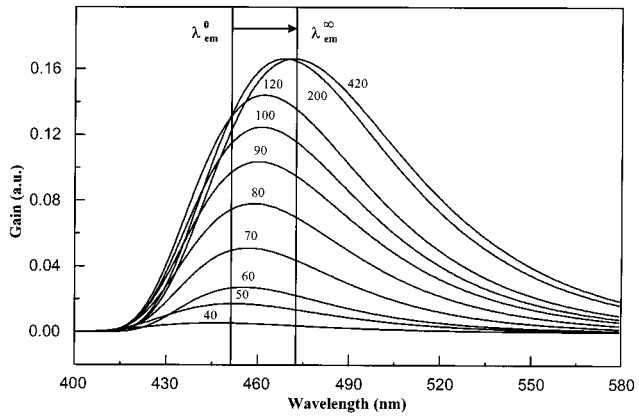

Figure 5. Time-resolved stimulated emission of C102 in 1-propanol solution from the log-normal treatment. Reported times are in ps. λ^0_{em} and λ^0_{em} correspond to stimulated emission maxima at the earliest stage of the solvation process and after, respectively.

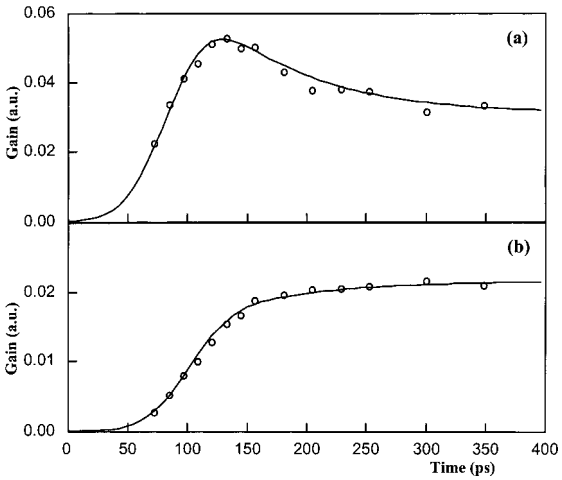

Figure 6. Kinetic treatment of the stimulated emission according to a biexponential fit. (a) Probed at 430 nm: $A = 0.031$; $B = 0.042$; $\sigma = 28$ ps; $\tau_1 \leq 5$ ps; $\tau_2 = 83 \pm 5$ ps; res(t) $= 3.96 \times 10^{-5}$. (b) Probed at 570 nm: $A = 0.0157$; $B = 0.059$; $\sigma = 28$ ps; $\tau_1 \leq 5$ ps; $\tau_2 = 83 \pm 5$ ps; res(t) $= 3.23 \times 10^{-6}$.

by transient absorption and can be fitted by a log-normal function even without any transient correction, as depicted in Figure 4.

The Stimulated Emission Band. An example of a typical stimulated emission series corrected from transient absorption and after log-normal analysis is shown in Figure 5 (C102 in 1-propanol), where the spectra have been inverted compared to Figure 1. After these corrections, one can analyze the time behavior of the stimulated emission; two examples are shown in Figure 6 where the emission is monitored at 430 nm (Figure 6a) and 570 nm (Figure 6b). However, these kinetics depend on two contributions: the build-up of the stimulated emission and the red shift of the emission maximum as a function of time. The contribution of the dynamic shift can be easily separated from the above kinetics by simply following the emission maximum as a function of time. The result is reported in Figure 7. This transient kinetic is fitted the same way as for the transient absorption (see relation 5). Then, the calculation yields a lifetime equal to 5 ps or less (time accuracy of the set up) that corresponds to the build-up of the stimulated process ($S_1 \rightarrow S_0$ transition). However, if we look to the stimulated emission spectra at pump−probe delays longer than 200 ps (not shown in Figure 5) the gain remains unchanged till 420 ps. Then, the apparent decay of emission (Figure 6a) is mainly due to the

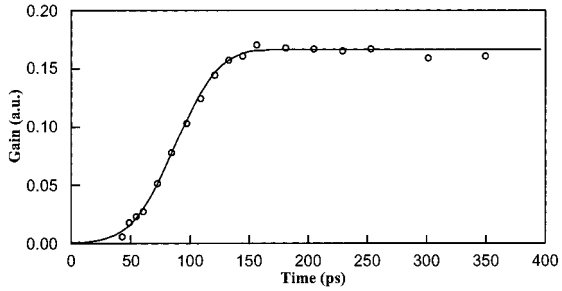

Figure 7. Kinetic treatment of the stimulated emission of C102 in 1-propanol corrected from the time dependent solvatochromic shift. Fitting parameters are $A = 0.166$; $\sigma = 28$ ps; $\tau \leq 5$ ps; res(t) $= 1.66 \times 10^{-4}$.

shift of the emission band. The same conclusion can be drawn for the apparent rise (Figure 6b) of the stimulated emission. From these observations, the best fit of data is a sum of two independent contributions: one corresponding to the build-up of the stimulated emission and the decay/rise of the stimulated emission caused by the shift of the emission band. According to the precedent result and observations, the kinetics in Figure 6 are analyzed by using a sum of two exponential functions: a short component with a lifetime equal to 5 ps (or less) corresponding to the stimulated emission build-up and a long component that is apparently correlated with the shift of the emission maximum. In the example of C102 in 2-propanol, a characteristic time of 83 ± 5 ps is found for the long component. The analysis of the stimulated emission in the other polar and hydroxylic solvents leads to the same conclusion: the stimulated emission and the dynamic shift are two independent processes. The nature of this dynamic shift will be discussed in the next section.

Apart from this dynamical aspect, there is no substructure in the stimulated emission band, as observed for C153 by Jiang et al.[23] with a similar time resolution. However, the time resolution of our device did not allow us to draw any conclusion regarding the role in the stimulated process of the excited electronic states in close energetic proximity.[23]

The Dynamic Solvatochromism of the Stimulated Emission Band. As reflected by Figure 5, the maximum of this band shifts to higher wavelengths as the pump−probe delay increases. This red shift is only observed for hydroxylic solvents 5−11, not for the others. For solvents 1−4, the solvation dynamics is faster than the time resolution of the apparatus. The dynamic studies will be limited to hydroxylic solvents 5−11 where the solvation is slow enough to be studied with the present time resolution. From the time-resolved stimulated emission spectra, one may try to extract the Stokes shift correlation function. At this point, one may define two quantities: (i) $\lambda_{em}{}^0$ (or $\bar{\nu}_{em}{}^0$) corresponds to the maximum of the stimulated emission when the overlap between the pump and probe pulses begins ($t \leq t_0$), and (ii) $\lambda_{em}{}^\infty$ (or $\bar{\nu}_{em}{}^\infty$) corresponds to the maximum of the stimulated emission from S_1 when most of the solvation process is achieved (i.e., when an appreciable shift is no longer observed), typically for a delay between the pump and probe pulses greater than 400 ps.

The maximum of the stimulated emission evolves from $\lambda_{em}{}^0$ to $\lambda_{em}{}^\infty$ as a function of time (Figure 5). These two wavelengths characterize the bathochromic shift.

The experimental values for the stimulated emission are reported in Table 1. As suggested by steady state solvent effect experiments, C102 is more sensitive to hydrogen bonding.[35] This specific interaction will certainly be reflected by the linear dependence of $\bar{\nu}_{em}{}^\infty$ toward the Dimroth polarity scale based

TABLE 1: Characteristics of C102 Stimulated Emission (see text)

	solvent	λ^0_{em} (nm)	λ^∞_{em} (nm)	$\bar{\nu}^0_{em}$ (nm)	$\bar{\nu}^\infty_{em}$ (nm)
1	acetone	460	460	21739	21739
2	DMF	463	463	21600	21600
3	DMSO	465	465	21505	21505
4	acetonitrile	463	463	21598	21598
5	2-propanol	448	468	22321	21368
6	1-butanol	460	474	21739	21097
7	1-propanol	452	473	22124	21142
8	ethanol	456	476	21930	21008
9	NMF	455	475	21978	21053
10	methanol	453	480	22075	20833
11	ethyleneglycol	455	485	21978	20619

TABLE 2: Various Solvent Parameters Used in Solvatochromic Studies

	solvent	$E_T(30)^a$	π^*	α	β
1	acetone	42.2	0.71	0.08	0.43
2	DMF	43.8	0.88	0.00	0.69
3	DMSO	45.1	1.00	0.00	0.76
4	acetonitrile	45.6	0.75	0.19	0.40
5	2-propanol	49.2	0.48	0.76	0.84
6	1-butanol	50.2	0.47	0.84	0.84
7	1-propanol	50.7	0.52	0.84	0.90
8	ethanol	51.9	0.54	0.86	0.75
9	NMF	54.1	0.90	0.62	0.80
10	Methanol	55.4	0.60	0.98	0.66
11	ethyleneglycol	56.3	0.92	0.90	0.52

[a] $E_T(30)$ in kcal mol^{-1}, π^*, α, and β from ref 60.

on the $E_T(30)$ solvent parameter[59] or the solvatochromic parameter approach[36−38,60] (Table 2).

From the results collected in Table 1, it is apparent that the maximum of the gain band evolves toward higher wavelengths as the polarity of the medium increases. A linear relationship is obtained between $\bar{\nu}_{em}^{\infty}$ and $E_T(30)$

$$\bar{\nu}_{em}^{\infty} = (24.8 \pm 0.3)10^3 - (72 \pm 6)\, E_T(30) \qquad r = 0.970\,,\ n = 11 \quad (7)$$

which denotes that hydrogen bonding is effective in the solvatochromism of the stimulated emission of C102. This result is also confirmed by a solvatochromic comparison method where a linear multiregression is found between the $\bar{\nu}_{em}^{\infty}$, π^*, and α parameters.

$$\bar{\nu}_{em}^{\infty} = (22.6 \pm 0.1)10^3 - (10.3 \pm 1.4)10^2\, \pi^* - (11.0 \pm 0.7)\, 10^2\, \alpha \quad (8)$$

where $r = 0.984$, $n = 11$, and π^* and α stand for the conventional electrostatic interaction (i.e., polarity/polarizability parameter), the hydrogen bond donation (HBD) ability to form a coordinative bond between the solvent and the solute, respectively. From this relationship, it is evident that the specific interactions play the same role as the dipolar ones since the numerical coefficients π^* and α are nearly equal (the ratio is close to unity). In other words, stabilization of the electronic state levels of C102 occurs with the same ratio through dipolar interactions and hydrogen bonding. Compared to the widely used C153 probe, which appears to be sensitive only to classical electrostatic interaction (see ref 29), coumarin dye C102, as a molecular probe, is more sensitive to hydrogen bond interaction.

The frequency $\bar{\nu}_{em}(t)$ corresponding to the gain band maximum at time t was determined from the displayed time-resolved spectra of the stimulated emission of C102 in 1-propanol (Figure 5). This last parameter must be defined as a characteristic frequency of the spectrum in order to measure the time-resolved solvatochromic shift described by the Stokes shift correlation function $C(t)$ given by the following expression:

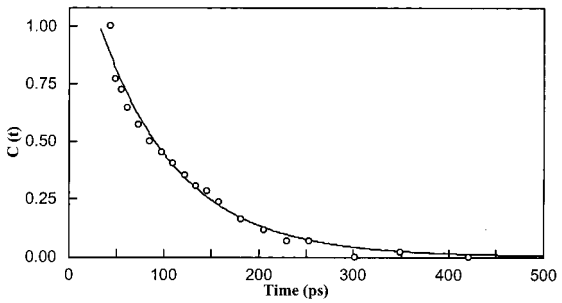

Figure 8. $C(t)$ function calculated for C102 in 1-propanol solution. This function is fitted by using a monoexponential decay with a characteristic lifetime of 83 ps.

TABLE 3: Dielectric Parameters and Kirkwood Factor of the Considered Solvents

solvent	ϵ_0	ϵ_∞	τ_D (ps)	n[e]	n^2	g_k[f]
5	19.40[b]	2.42[b]	359[b]	1.3752	1.891	2.27
6	18.38[d]	2.72[d]	528.4[d]	1.3974	1.953	2.48
7	20.43[b]	2.44[b]	329[b]	1.3837	1.915	2.28
8	24.32[b]	2.69[b]	163[b]	1.3594	1.848	2.15
9	183.3[a]	3.2[a]	128[a]	1.4300	2.050	4.40
10	32.5[b]	2.79[b]	51.5[b]	1.3265	1.760	2.20
11	41.65[c]	3.95[c]	122.5[c]	1.4306	2.047	2.89

[a] Reference 65. [b] Reference 66. [c] Reference 67. [d] Reference 68. [e] Reference 69. [f] Reference 72 except for solvents 9 and 11 calculated from formula in the same paper.

$$C(t) = \frac{\bar{\nu}_{em}(t) - \bar{\nu}_{em}^{\infty}}{\bar{\nu}_{em}^{0} - \bar{\nu}_{em}^{\infty}} \quad (9)$$

Generally, this function, which may be fitted with a monoexponential decay curve, yields a characteristic time for the dynamic shift. To measure this characteristic time more accurately, $\bar{\nu}_{em}(t)$ was determined by fitting the transient spectrum, especially in the very first stage of the experiment ($t \le t_0$), with a log-normal shape function $\epsilon(\nu)$ as defined by ref 57. This procedure was applied for all the solvents and shown as an example in Figure 8 for C102 in 1-propanol solution. It is apparent that, in this particular case, the shift concerned with the solvation process occurs in a few tens of picoseconds.

Discussion

All the data obtained with C102 are collected in Table 4 together with the experimental results derived from research work dealing with probe molecules such as C153,[29] MPQB,[16] and thioxanthone (TX).[45] The two last molecules are hydrogen bond sensitive probes. Some characteristic solvation times of the solvent were added. The Debye relaxation time τ_D (or the bulk dielectric relaxation time of the solvent), which involves the response of all solvent molecules, correlated to each together. The longitudinal relaxation time, τ_L, is expressed from the Debye continuum theory[4,7,8,62,63] as

$$\tau_L = \frac{2\epsilon_\infty + 1}{2\epsilon_0 + 1}\tau_D \quad (10)$$

and often used in the well-known reduced form

$$\tau_L \approx \frac{\epsilon_\infty}{\epsilon_0}\tau_D \quad (11)$$

where ϵ_∞ and ϵ_0 are the dielectric constants of the solvent in an electric field of infinite frequency and in a static field, respectively.

TABLE 4: Molecular Relaxation Times

	measured relaxation time τ (ps)				solvent relaxation time (ps)		
solvent	C102[a]	C153[b]	MPQB[c]	TX[d]	τ_D	τ_L	τ_M
5	79			95	359	42	110.3
6	123	63.00 (133)		120	528.4	68.6	149.5
7	83	26.00 (47.8)		90	329	38	100.7
8	61	16.00 (29.6)	41	72	163	15.4	52.4
9	37	5.70 (53.4)		55	128	1.8	19.5
10	12	5.00 (15.3)	< 40	20	51.5	3.5	16
11	51	15.30 (32)	52	80	122.5	7.4	29

[a] Our results. [b] Average time (in parentheses the longest time) of the multiexponential fit as defined in Reference 29. [c] Reference 16. [d] Reference 45.

The microscopic or molecular relaxation time, τ_M, corresponds to a theoretical approach (which applies to cage relaxation dynamics) and was developed by Kivelson et al.[64,65] These authors studied the polarization of a dipolar solvent by a dipole (or an ion) suddenly created in the bulk. Two distinct regions are considered: "the low k limit" far away from the dipole where the solvent relaxes with the longitudinal time τ_L as in other continuum models, and the "high k limit" near the dipole where the interactions between the solvent molecules and the dipoles are so strong that the correlation between the solvent molecules is lost. Thus, the solvent molecules individually relax, without correlation, with a characteristic time τ_M[15−17,64,65] given by

$$\tau_M = \left[\frac{2\epsilon_0 + \epsilon_\infty}{3\epsilon_0 g_k}\right]\tau_D \qquad (12)$$

where g_k is the Kirkwood factor of the solvent ,which reflects the degree of short range order in the liquid (the degree of association). This characteristic time τ_M is a molecular property where a single solvent molecule relaxes individually around the solute one. A different formalism used by Maroncelli et al.[33] leads to an equivalent expression for τ_M, stressing the importance of the Kivelson formalism.

Therefore, τ_M and τ_L can be calculated from a set of macroscopic data (ϵ_∞, ϵ_0, τ_D, g_k). The dielectric parameters ϵ_∞, ϵ_0, and τ_D are obtained from dielectric relaxation measurements (see references in Table 3) and can be used to calculate the τ_L relaxation times (Table 4). However, it was pointed out that the best value for ϵ_∞ is n^2, where n is the refractive index of the medium as established by several authors.[15,71,72] The last parameter, the Kirkwood factor g_k, was obtained from ref 73 except for solvents 9 and 11, in which case $g_k$was calculated from the formula reported by Jay-Gerin et al.[73] and by using the dielectric data in Table 3. Finally, the microscopic (single-particle) relaxation time τ_M was estimated by using the set of values ($\epsilon_\infty = n^2$, ϵ_0, τ_D, g_k) shown in Table 3.

A glance at Table 4, collecting all the characteristic relaxation times and the experimental values obtained by using C153 as a probe,[29] shows that the relaxation times measured by using the C102 as a probe are generally longer than the longitudinal relaxation time τ_L and closer to the calculated single-particle relaxation time, τ_M. As reported in ref 29, the experimental relaxation times for C153 are very close to the longitudinal relaxation ones, which reflect the fact that the related solvation process is mainly due to dipolar interactions. The other significant fact is that the present relaxation times obtained with C102 as a probe are in good agreement with the molecular relaxation times τ (Table 4) recorded for two hydrogen-bond sensitive probes, MPQB[16] and more recently TX.[45] For MPQB, Rullière et al.[16] show that the relaxation times reported in Table 4 correspond to the appearance of a specific interaction with a solvent molecule. In the case of TX, the results lead to the conclusion that the major solvation process around this probe is produced by hydrogen bonding.[45] In addition Yu et al.[20] report a hydrogen bonding time of 65 ps in ethanol by using Resorufin as a probe, which is in good agreement with the 61 ps measured in the present work.

It was reported[74] that C102 forms weak but distinct complexes with hydroxylic solvents, such as methanol and 1-butanol, in both the ground and excited singlet states. In that study,[74] the data were analyzed in terms of decay associated fluorescence spectra (DAS), which can reveal a kinetic correlation between the initial excited state and the final solvent equilibrated state.

Among these results, the data obtained in methanol and 1-butanol are of particular interest, especially the observed short component with lifetimes equal to 22 and 109 ps, respectively. These measured values are in good agreement with the one concerning the dynamic red shift of the stimulated emission and obtained through pump−probe spectroscopy (see Table 4). This supports the idea of hydrogen bonding between solute C102 and one molecule of solvent, as already mentioned in the solvatochromism of TX,[45] C153 in methanol,[30] and in papers by Nibbering et al.[41−44] regarding hydrogen bonding between C102 and hydrogen donor. This bonding leads to the formation of a complex between the probe in the excited singlet state and the hydroxylic solvent. As the measured relaxation times generally fall in the limited range $\tau_L < \tau < \tau_M$ and from earlier results for a well characterized polar probe MPQB,[17] one may suggests two main relaxation mechanisms of polar solvents expressing the low-frequency part of the solvation dynamics.[17,22,71] These mechanisms are (i) the collective reorientation of solvent molecules in weak interactions with the probe, scaled by the (macroscopic) longitudinal relaxation time of the solvent, τ_L, as defined by relation 10, and (ii) the individual reorientation of the solvent molecules in strong interaction with the probe (including, tentatively, complex formation such as H-bonding), scaled by microscopic (single-particle) reorientation time, τ_M, as defined by relationship (12). It is possible to conclude that the solvation times observed in the present study result from hydrogen bonding between C102 and one solvent molecule. Thus, the solvation around C102 is mainly microscopic in nature with a characteristic time equivalent to the microscopic relaxation time τ_M. At a shorter time scale, the solvation process is mainly dipolar in nature. This shows that specific interactions lead to longer relaxation times than classical dipolar interactions, as already observed for other molecular probes.[15−18]

Conclusion

The solvatochromism of the stimulated emission of a coumarin derivative C102 was investigated in several solvents. This solvatochromism cannot only be described through classical dipolar interactions (dielectric continuum model) since this kind

of interaction occurs at shorter time scale but also in terms of molecular relaxation or, in other words, by hydrogen bonding interaction. This is consistent with the above results, $E_T(30)$, the Kamlett and Taft linear correlations (SCM method) for the stimulated emission, where it was demonstrated that the hydrogen bonding interaction plays a major role in the dynamic solvatochromism of dye C102. This study leads us to the conclusion that the first excited-state level, S_1, is equally stabilized by dipolar and specific interactions, especially the H-bonding.

The pump−probe technique was used to characterize the transient absorption and the stimulated emission with a higher resolution compared to other techniques, such as photon counting. From this dynamical study, the emission arises from a unique singlet excited state and there is no substructure in the emission band. This last result is different from what was reported by Jiang et al.[23] for C153. However, the time resolution of the present technique did not allow any conclusion regarding the intramolecular energy dissipation characteristics.

In addition, the dynamic solvatochromism in hydroxylic solvents was taken into account. The measured relaxation times τ derived from spectral analysis are centered around τ_M and are significantly different from τ_L and τ_D. The relaxation times τ measured for C102 in its excited singlet state are almost the same as those measured for TX in its first excited triplet state. It means that the nature of the excited state did not play any role in the solvent−solute relaxation. It is possible to conclude that the solvation times τ observed in the present study result from hydrogen bonding between C102 and one solvent molecule. Thus, the solvation around C102 is mainly microscopic in nature with a characteristic time equivalent to the microscopic relaxation time τ_M.

References and Notes

(1) Barbara, P. F.; Jarzeba, W. *Adv. Photochem.* **1990**, *15*, 1.
(2) Simon, J. D. *Acc. Chem. Res.* **1988**, *21*, 128.
(3) Maroncelli, M. *J. Mol. Liq.* **1993**, *57*, 1.
(4) Mazurenko, Yu. T. *Opt. Spectrosc.* **1974**, *36*, 283.
(5) Bakshiev, N. G. *Opt. Spectrosc. (USSR)* **1964**, *16*, 446.
(6) Mazurenko, Yu. T.; Bakshiev, N. G. *Opt. Spectrosc. (USSR)* **1970**, *28*, 490.
(7) Bagchi, B.; Oxtoby, D. W.; Fleming, G. R. *Chem. Phys.* **1984**, *86*, 257.
(8) van der Zwan, G.; Hynes, J. T. *J. Phys. Chem.* **1985**, *89*, 4181.
(9) Maroncelli, M.; Kumar, V. P.; Papazyan, A. *J. Phys. Chem.* **1993**, *97*, 13.
(10) Mataga, N.; Kubota, T. *Molecular Interactions and Electronic Spectra*; Marcel Dekker: New York, 1970.
(11) Berg, M. *J. Phys. Chem. A* **1998**, *102*, 17.
(12) Fourkas, J. T.; Berg, M. *J. Chem. Phys.* **1993**, *98*, 7773.
(13) Fourkas, J. T.; Benigno, A.; Berg, M. *J. Chem. Phys.* **1993**, *99*, 8552.
(14) Struve, W. S.; Rentzepis, P. M. *Chem. Phys. Lett.* **1974**, *29*, 23.
(15) Declémy, A.; Rullière, C. *AIP Conf. Proc.* **1994**, *298*, 275.
(16) Declémy, A.; Rullière, C.; Kottis, P. *Laser Chem.* **1990**, *10*, 413.
(17) Declémy, A.; Rullière, C. *Chem. Phys. Lett.* **1988**, *146*, 1.
(18) Declémy, A.; Rullière, C.; Kottis, P. *Chem. Phys. Lett.* **1987**, *133*, 448.
(19) Anthon, D. W.; Clark, J. H. *J. Phys. Chem.* **1987**, *91*, 3530.
(20) Yu, J.; Berg, M. *Chem. Phys. Lett.* **1993**, *208*, 315.
(21) Agmon, N. *J. Phys. Chem.* **1990**, *94*, 2959.
(22) Maroncelli, M.; Fleming, G. R. *J. Chem. Phys.* **1987**, *86*, 6221.
(23) Jiang, Y.; McCarthy, P. K.; Blanchard, G. J. *Chem. Phys.* **1994**, *183*, 249.
(24) Kovalenko, S. A.; Ruthmann, J.; Ernsting, N. P. *Chem. Phys. Lett.* **1997**, *271*, 40.
(25) McCarthy, P. K.; Blanchard, G. J. *J. Phys. Chem.* **1993**, *97*, 12205.
(26) Bingemann, D.; Ernsting, N. P. *J. Chem. Phys.* **1995**, *102*, 2691.
(27) Kovalenko, S. A.; Ernsting, N. P.; Ruthmann, J. *J. Chem. Phys.* **1997**, *106*, 3504.
(28) Pollard, W. T.; Mathies, R. A. *Annu. Rev. Phys. Chem.* **1992**, *43*, 497.
(29) Horng, M. L.; Gardecki, J. A.; Papazyan, A.; Maroncelli, M. *J. Phys. Chem.* **1995**, *99*, 17311.
(30) Gustavsson, T.; Cassara, L.; Gulbinas, V.; Gurzadyan, G.; Mialocq, J.-C.; Pommeret, S.; Sorgius, M.; van der Meulen, P. *J. Phys. Chem. A* **1998**, *102*, 4229.
(31) Maroncelli, M.; Fee, R. S.; Chapman, C. F.; Fleming, G. R. *J. Phys. Chem.* **1991**, *95*, 1012.
(32) Kahlow, M. A.; Kang, T. J.; Barbara, P. F. *J. Chem. Phys.* **1988**, *88*, 2372.
(33) Chapman, C. F.; Fee, R. S.; Maroncelli, M. *J. Phys. Chem.* **1990**, *94*, 4929.
(34) Jones, G., II; Jackson, W. R.; Choi Chol-yoo; Bergmark, W. R. *J. Phys. Chem.* **1985**, *89*, 294.
(35) Moog, R. S.; Davis, W. W.; Ostrowsky, S. G.; Wilson, G. L. *Chem. Phys. Lett.* **1999**, *299*, 265.
(36) Kamlet, M. J.; Taft, R. W. *J. Am. Chem. Soc.* **1976**, *98*, 377.
(37) Taft, R. W.; Kamlet, M. J. *J. Am. Chem. Soc.* **1976**, *98*, 2886.
(38) Kamlet, M. J.; Abboud, J. L. M.; Abraham, M. H.; Taft, R. W. *J. Org. Chem.* **1983**, *48*, 2877.
(39) Suppan, P. *J. Photochem. Photobiol. A*: *Chem.* **1990**, *50*, 293.
(40) Zewail, A. H. *J. Phys. Chem.* **1996**, *100*, 12701.
(41) Tschirschwitz, F.; Nibbering, E. T. J. *Chem. Phys. Lett.* **1999**, *312*, 169.
(42) Nibbering, E. T. J.; Tschirschwitz, F.; Chudoba, C.; Elsaesser, T. *J. Phys. Chem. A* **2000**, *104*, 4236.
(43) Chudoba, C.; Nibbering, E. T. J.; Elsaesser, T. *J. Phys. Chem. A* **1999**, *103*, 5625.
(44) Nibbering, E. T. J.; Chudoba, C.; Elsaesser, T. *Isr. J. Chem.* **1999**, *39*, 333.
(45) Morlet-Savary, F.; Ley, C.; Jacques, P.; Wieder, F.; Fouassier, J. P. *J. Photochem. Photobiol., A*: *Chem.* **1999**, *126*, 7.
(46) Samanta, A.; Fessenden, R. W. *J. Phys. Chem. A* **2000**, *104*, 8577.
(47) Kumar, P. V.; Maroncelli, M. *J. Chem. Phys.* **1995**, *103*, 3038.
(48) Diraison, M.; Millié P.; Pommeret, S.; Gustavsson, T.; Mialocq, J. C. *Chem. Phys. Lett.* **1998**, *282*, 152.
(49) Mühlpfordt, A.; Schanz, R.; Ernsting, N. P.; Farztdinov, V.; Grimme, S. *Phys. Chem. Chem. Phys.* **1999**, *1*, 3209.
(50) Cichos, F.; Brown, R.; Rempel, U.; von Borczyskowski, C. *J. Phys. Chem. A* **1999**, *103*, 2506.
(51) Lopez Arbeloa, T.; Lopez Arbeloa, F.; Tapia, M. J.; Lopez Arbeloa, I. *J. Phys. Chem.* **1993**, *97*, 4704.
(52) Priyadarsini, K. I.; Naik, D. B.; Moorthy, P. N. *J. Photochem. Photobiol. A*: *Chem.* **1989**, *46*, 239.
(53) Priyadarsini, K. I.; Naik, D. B.; Moorthy, P. N. *Chem. Phys. Lett.* **1989**, *157*, 525.
(54) Priyadarsini, K. I.; Naik, D. B.; Moorthy, P. N. *J. Photochem. Photobiol. A*: *Chem.* **1990**, *54*, 251.
(55) Dempster, D. N.; Morrow, T.; Quinn, M. F. *J. Photochem.* **1973**−**74**, *2*, 329.
(56) Yip, R. W.; Wen, Y. X. *J. Photochem. Photobiol. A*: *Chem.* **1990**, *54*, 263.
(57) Siano, D. B.; Metzler, D. E. *J. Chem. Phys.* **1969**, *51*, 1856.
(58) Morlet-Savary, F.; Jacques, P.; Fouassier, J. P., in preparation.
(59) Reichardt, C. *Solvents and solvent effects in organic chemistry*; VCH: Weinheim, 1988.
(60) Buncel, E.; Rajagopal, S. *Acc. Chem. Res.* **1990**, *23*, 226.
(61) Marcus, Y. *Chem. Soc. Rev.* **1993**, 409.
(62) Böttcher, C. J. F.; Bordewijk, P. *Theory of electric polarization*; Elsevier: Amsterdam, 1977; Vol. I.
(63) Frölich, H. *Theory of Dielectrics*, 2nd ed.; Oxford University Press: Oxford, 1958.
(64) Madden, P.; Kivelson, D. *Adv. Chem. Phys.* **1984**, *56*, 467.
(65) Friedrich, V.; Kivelson, D. *J. Chem. Phys.* **1987**, *86*, 6425.
(66) Barthel, J.; Bachhuber, K.; Buchner, R.; Gill, J. B.; Kleebauer, M. *Chem. Phys. Lett.* **1990**, *167*, 62.
(67) Barthel, J.; Bachhuber, K.; Buchner, R.; Hetzenauer, H. *Chem. Phys. Lett.* **1990**, *165*, 369.
(68) Jordan, B. P.; Sheppard, R. J.; Szwarnowski, S. *J. Phys. D* **1978**, *11*, 695.
(69) Mashimo, S.; Kuwabara, S.; Yagihara, S.; Higasi, K. *J. Chem. Phys.* **1989**, *90*, 3292.
(70) Riddick, J. A.; Bunger, W. B.; Sakano, T. K. *Organic Solvents*; Wiley: New York, 1986.
(71) Castner, E. W.; Maroncelli, M.; Fleming, G. R. *J. Chem. Phys.* **1987**, *86*, 1090.
(72) Sumi, H.; Marcus, R. A. *J. Chem. Phys.* **1986**, *84*, 4272.
(73) Jay-Gerin, J. P.; Ferradini, C. *Radiat. Phys. Chem./Int. J. Radiat. Appl. Instrum., C.* **1990**, *36*, 317.
(74) Yip, R. W.; Wen, Y. X. *Can. J. Chem.* **1991**, *69*, 1413.